Functional Necessity and Physicochemical Characteristics of the [2Fe−2S] Cluster in Mammalian Ferrochelatase

Steven G. Lloyd,[†] Ricardo Franco,[§,||] José J. G. Moura,[‡] Isabel Moura,*[,‡] Glória C. Ferreira,*[,§] and Boi Hanh Huynh*[,†]

Contribution from the Department of Physics, Emory University, Atlanta, Georgia 30322, the Departamento de Química (and the Centro de Química Fina e Biotecnologia), Faculdade de Ciências e Tecnologia, Universidade Nova de Lisboa, 2825 Monte de Caparica, Portugal, and the Department of Biochemistry and Molecular Biology, College of Medicine, Institute for Biomolecular Science, H. Lee Moffit Cancer Center and Research Institute, University of South Florida, Tampa, Florida 33612

Received November 28, 1995[⊗]

Abstract: The recently discovered [2Fe−2S] cluster in mouse liver ferrochelatase has been characterized using UV−vis, EPR, and Mössbauer spectroscopic techniques. Studies are reported here for the recombinant protein purified from an overproducing transformed *Escherichia coli* strain. A positive correlation is observed between the presence of the [2Fe−2S] cluster and the enzymatic specific activity and demonstrates the necessity of this cofactor. Chemical analysis revealed that the preparations contained up to 1.3 Fe/molecule and indicated a 1:1 stoichiometry between Fe and acid−labile sulfide. The [2Fe−2S] cluster in the as-isolated ferrochelatase exhibits a UV−vis spectrum indicative of a $[2Fe-2S]^{2+}$ cluster and is EPR-silent. The 8 T Mössbauer spectrum of the ^{57}Fe-enriched as-isolated protein is well simulated by parameters $\Delta E_Q = 0.69 \pm 0.03$ mm/s and $\delta = 0.28 \pm 0.02$ mm/s and confirms the presence of a diamagnetic ground state. Upon reduction with sodium dithionite, ferrochelatase shows a near-axial EPR spectrum with g-values of 2.00, 1.93, and 1.91, consistent with a $S = {}^1/_2$ mixed valent $Fe^{3+}-Fe^{2+}$ cluster. The Orbach temperature dependence of the EPR line widths was used to provide an estimate of the exchange coupling J, which was determined to be on the order of 500−650 cm^{-1} ($+J\mathbf{S}_1\cdot\mathbf{S}_2$ model). Redox titrations monitored by UV−vis and EPR spectroscopy revealed midpoint potentials of -390 ± 10 and -405 ± 10 mV, respectively. Mössbauer spectra of the sodium dithionite-reduced ^{57}Fe-enriched ferrochelatase collected at 4.2 K in the presence of magnetic fields of 60 mT and 8 T strengths were analyzed in the mixed-valent $S = {}^1/_2$ ground state. Parameters for the ferric site are $\Delta E_Q = 1.2 \pm 0.2$ mm/s and $\delta = 0.28 \pm 0.03$ mm/s, with somewhat anisotropic hyperfine splittings; for the ferrous site, $\Delta E_Q = 3.3 \pm 0.1$ mm/s and $\delta = 0.67 \pm 0.04$ mm/s with anisotropic hyperfine splittings characteristic of high-spin ferrous ion. The similarities and differences with other characterized $[2Fe-2S]^+$ cluster-containing proteins are discussed.

Introduction

Ferrochelatase (EC 4.99.1.1), the terminal enzyme in the heme biosynthetic pathway, catalyzes the insertion of ferrous ion into protoporphyrin IX to form protoheme. *In vitro*, it is also known to utilize a variety of divalent metal ions and porphyrin isomers as substrates.[1,2] Moreover, certain divalent metals (*e.g.*, Mn^{2+}, Hg^{2+}, and Cd^{2+})[3] and porphyrin derivatives (*e.g.*, *N*-methylprotoporphyrin IX)[4] are known to be potent inhibitors of the enzyme. Because hemes are among the most ubiquitous and essential of cofactors, an understanding of the control, regulation, and molecular mechanism of ferrochelatase activity is crucial.

Recently, our work with recombinant mouse liver ferrochelatase led to the discovery of a [2Fe−2S] cluster in this protein.[5] The recombinant enzyme is found associated with the bacterial soluble fraction and hence is quite amenable to spectroscopic investigation. The EPR spectrum of the as-isolated protein showed no resonances, while the sodium dithionite-reduced protein demonstrated resonances typical of a $S = {}^1/_2$ system. Mössbauer spectra of the ^{57}Fe-enriched enzyme were similar to those of other well-characterized [2Fe−2S] clusters. EPR spectroscopy confirmed that the cluster also exists in ferrochelatase purified directly from mouse liver. The cluster was found to exist in substoichiometric amounts, occurring in the range of 0.2−0.5 cluster/molecule. A cluster of this type, in quantities up to 0.5−1 cluster/protein, was also found in recombinant human ferrochelatase;[6] the cluster in the human protein, however, was reported to be very unstable.

The ferrochelatase gene has been isolated, cloned, and sequenced from several organisms.[1] Of all the species whose ferrochelatase genes have been sequenced to date, only the mammalian enzymes (mouse,[7] bovine,[8] and human[9]) have conserved cysteine residues. Four of the conserved cysteines

* Authors to whom correspondence should be addressed.
[†] Emory University.
[‡] Universidade Nova de Lisboa.
[§] University of South Florida.
[||] Present address: Departamento de Química, Faculdade de Ciências e Tecnologia, Universidade Nova de Lisboa, 2825 Monte de Caparica, Portugal.

[⊗] Abstract published in *Advance ACS Abstracts,* October 1, 1996.

(1) Ferreira, G. C.; Franco, R.; Lloyd, S. G.; Moura, I.; Moura, J. J. G.; Huynh, B. H. *J. Bioenerg. Biomembr.* **1995**, *27*, 221−229.
(2) Dailey, H. A. In *Biosynthesis of Heme and Chlorophylls*; Dailey, H. A., Ed.; McGraw-Hill Publishing Co.: New York, 1990; pp 123−161.
(3) Dailey, H. A. *Ann. N.Y. Acad. Sci.* **1987**, *514*, 81−86.
(4) Lavallee, D. K. *The Chemistry and Biochemistry of N-Substituted Porphyrins*; VCH Publishers: New York, 1987; pp 181−207.
(5) Ferreira, G. C.; Franco, R.; Lloyd, S. G.; Pereira, A. S.; Moura, I.; Moura, J. J. G.; Huynh, B. H. *J. Biol. Chem.* **1994**, *269*, 7062−7065.
(6) Dailey, H. A.; Finnegan, M. G.; Johnson, M. K. *Biochemistry* **1994**, *33*, 403−407.
(7) Taketani, S.; Nakahashi, Y.; Osumi, T.; Tokunaga, R. *J. Biol. Chem.* **1990**, *265*, 19377−19380.
(8) Shibuya, H.; Nonneman, D.; Tamassia, M.; Allphin, O. L.; Johnson, G. S. *Biochim. Biophys. Acta* **1995**, *1231*, 117−120.
(9) Nakahashi, Y.; Taketani, S.; Okuda, M.; Inoue, K.; Tokunaga, R. *Biochem. Biophys. Res. Commun.* **1990**, *173*, 748−755.

S0002-7863(95)04000-5 CCC: $12.00

in the mammalian proteins are found in a 30-residue C-terminus tail that is lacking in the prokaryotic enzymes (the plant ferrochelatase genes and the ferrochelatase gene of the yeast *Saccharomyces cerevisiae* encode a C-terminus tail but do not encode the mammalian conserved cysteines).[1] Significantly, these cysteines are found in a sequence Cys-X_7-Cys-X_2-Cys-X_4-Cys that is suggestive of a [2Fe−2S]-binding motif.[10] The UV−vis spectrum of wild-type human recombinant ferrochelatase, although partially obscured by the presence of a heme contaminant, demonstrated bands at 330, 460, and 550 nm typical of $[2Fe-2S]^{2+}$ cluster-containing proteins, while the spectra of *S. cerevisiae* and *Escherichia coli* ferrochelatases lacked such bands, as did a truncated human ferrochelatase in which the 30-residue C-terminus tail had been deleted.[6] When the wild-type human ferrochelatase was stored at 4 °C, the UV−vis bands gradually disappeared. Interestingly, it was reported that as these bands were lost, ferrochelatase activity was lost concomitantly. The truncated human ferrochelatase was also reported to have no activity. On the basis of these observations it was proposed that the [2Fe−2S] cluster is necessary for activity in this enzyme.

Although these findings suggest that the [2Fe−2S] cluster is in some way necessary for ferrochelatase activity in the mammalian enzymes, the exact role of the clusters has yet to be defined. Its function could be regulatory, catalytic, structural, redox-related, or some combination of these. In a recent report, biochemical techniques and UV−vis spectroscopy were used to indicate that nitric oxide (NO) reacts with ferrochelatase, inactivating the enzyme and probably destroying the [2Fe−2S] cluster.[11] It is not surprising that NO reacts with the ferrochelatase cluster, since this small molecule is known to react with many Fe-containing moieties in biological compounds and model complexes.[12] NO is a well-established intercellular signal compound, however,[13] and therefore Furukawa *et al*.[11] postulated that this reaction might be a means of physiologic regulation of ferrochelatase activity. Further studies of this type, using complementary biochemical and spectroscopic methods, will help in achieving a full understanding of the role of the ferrochelatase [2Fe−2S] cluster. Comparative studies utilizing site-directed ferrochelatase mutants and non-cluster-containing (*i.e.*, nonmammalian) ferrochelatases will also aid in this understanding. Recently, we reported the characteristics of the metal substrate binding site as determined by Mössbauer spectroscopy and biochemical techniques.[14] We found that the protein ligands to the iron substrate are derived from nitrogen/oxygen species and ruled out contribution of sulfur ligands. We next turned to studies of the function of the [2Fe−2S] cluster in the enzyme.

Our study of the [2Fe−2S] cluster is motivated by data presented here that establish a positive correlation between the presence of the cluster and ferrochelatase specific activity. As a first step toward elucidating the function of the $[2Fe-2S]^{2+/+}$ cluster in recombinant murine ferrochelatase, we have characterized its physicochemical properties in detail using UV−vis, EPR, and Mössbauer spectroscopies and chemical analysis. Interesting differences and similarities between this cluster and others in its class have emerged from these findings. These results also provide base line information necessary for examination of the cluster status during catalytic turnover and any possible regulatory processes.

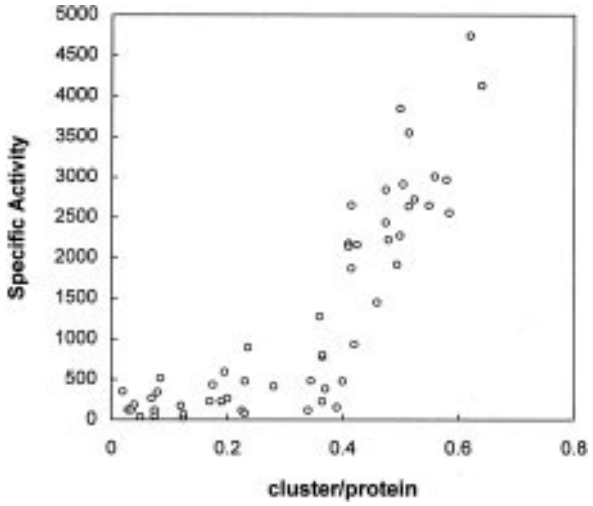

Figure 1. Specific activity *vs* cluster content per protein for different ferrochelatase chromatographic fractions. Each active fraction with a detectable visible absorbance at 440 nm was individually tested. Activity experiments and protein and iron determinations were carried out as described in the Experimental Section. Specific activity units are nanomoles of deuteroheme produced per minute per milligram of protein.

Results

Functional Necessity of the [2Fe−2S] Cluster. A question that arose immediately with the discovery of the [2Fe−2S] cluster in the mammalian ferrochelatases is whether the cluster is needed for activity. We have found that, within the chromatographic elution profile of mouse ferrochelatase, the fractions exhibiting ferrochelatase activity do not all have the same Fe:protein ratio (as judged by chemical iron analysis, see below). Rather, there is a distribution of this Fe:protein ratio, and therefore by selecting the appropriate fractions, we can achieve some control of the iron content in the enzyme preparations. Furthermore, $[2Fe-2S]^{2+}$ clusters are known to have UV−vis resonances at 440 nm.[15−18] Importantly, the ratio A_{440}/[Fe] is a constant (data not shown), indicating that all of the iron present in these protein samples is in the form of the [2Fe−2S] cluster (see below) and ruling out the presence of adventitious iron. These findings have allowed us to study ferrochelatase specific activity as a function of cluster content. A positive correlation has been definitively established between the presence of the [2Fe−2S] cluster in ferrochelatase chromatographic fractions and the specific activity of the fraction (Figure 1). At low cluster:protein ratios (below about 0.35), the specific activity is essentially constant. At ratios above 0.35, however, the specific activity increases very rapidly. This interesting cluster-dependent behavior is not well understood at present, but the nonlinear nature of the relationship may indicate that the active enzyme has a multimeric structure. The data do, however, establish that the presence of the cluster is necessary for ferrochelatase activity in the mouse protein. As a first step toward examining the role of the cluster in regulation and/or catalysis, we have characterized its chemical and physical properties.

(10) Cammack, R. In *Advances in Inorganic Chemistry*; Sykes, A. G., Ed.; Academic Press: New York, 1992; Vol. 38, pp 281−322.
(11) Furukawa, T.; Kohno, H.; Tokunaga, R.; Taketani, S. *Biochem. J.* **1995**, *310*, 533−538.
(12) Butler, A. R.; Glidewell, C.; Li, M.-H. In *Advances in Inorganic Chemistry*; Sykes, A. G., Ed.; Academic Press: New York, 1988; Vol. 32, pp 335−393.
(13) Stamler, J. S.; Singel, D. J.; Loscalzo, J. *Science* **1992**, *258*, 1898−1902.
(14) Franco, R.; Moura, J. J. G.; Moura, I.; Lloyd, S. G.; Huynh, B. H.; Forbes, W. S.; Ferreira, G. C. *J. Biol. Chem.* **1995**, *270*, 26352−26357.
(15) Armengaud, J.; Meyer, C.; Jouanneau, Y. *Biochem. J.* **1994**, *300*, 413−418.
(16) Ta, D. T.; Vickery, L. E. *J. Biol. Chem.* **1992**, *267*, 11120−11125.
(17) Palmer, G. In *Iron-Sulfur Proteins*; Lovenberg, W., Ed.; Academic Press: Orlando, FL, 1973; Vol. 2, pp 285−325.
(18) Cardenas, J.; Mortenson, L. E.; Yoch, D. C. *Biochim. Biophys. Acta* **1976**, *434*, 244−257.

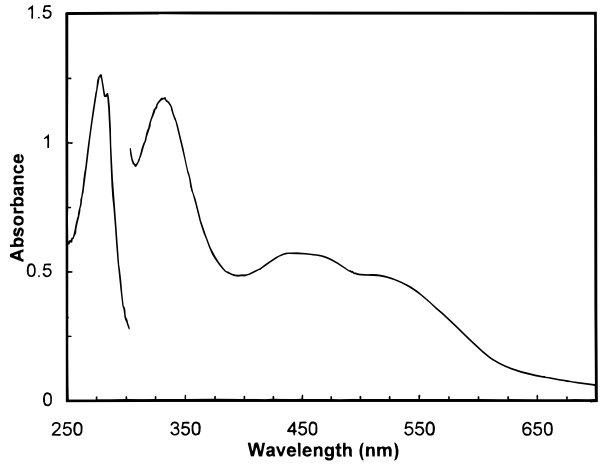

Figure 2. UV−vis spectra of the native ferrochelatase. Conditions: protein concentration, 12.5 μM for 250−300 nm, 50 μM for 300−700 nm; 1 cm path length quartz cuvette; protein in a 20 mM Tris·HCl, pH = 8.0 buffer containing 10% glycerol, 1% sodium cholate, and 1.5 M NaCl.

Chemical Analysis. Chemical analyses of the recombinant ferrochelatase were conducted in order to determine iron and labile sulfide content and thus verify the composition of the cluster. When all fractions from the blue Sepharose chromatography column that exhibited ferrochelatase activity were pooled, the average iron and acid-labile sulfide contents were determined to be 0.7 ± 0.2 Fe/molecule and 0.6 ± 0.2 S^{2-}/molecule, respectively, consistent with the stoichiometry expected for proteins containing a [2Fe−2S] cluster. It should be noted that SDS-PAGE (sodium dodecyl sulfate polyacrylamide gel electrophoresis) analysis of all purified ferrochelatase fractions demonstrated only a single band at 42 500 Da, signifying that the protein was purified to homogeneity.[19] The substoichiometric results of the elemental analysis therefore indicate that the chromatography fractions are an inhomogeneous mixture of apoprotein and holoprotein. When the iron content of the central fractions of the elution was measured, it was found that certain fractions contained as much as 1.44 Fe/protein by TPTZ (2,4,6-tripyridyl-(*S*)-triazine colorimetric analysis (see Experimental Section). Substoichiometric quantities of iron and low EPR spin quantitation were reported previously for both the wild-type recombinant and native mouse proteins.[5] The current results suggest that up to at least 70% pure holoprotein can be obtained by appropriate selection of the chromatography fractions.

UV−Visible Spectroscopy. $[2Fe-2S]^{2+}$ clusters exhibit distinct UV−vis spectra.[15−18] Figure 2 shows the UV−vis spectrum of the as-isolated recombinant mouse enzyme collected from the elution fractions containing the highest Fe content (1.44 Fe/protein). The protein absorption band in the UV region is a double peak with maxima at 285 and 278 nm. The spectrum has an absorption band at 330 nm [$\epsilon \approx 22\,000$ (M ferrochelatase)$^{-1}$ cm^{-1}] with prominent shoulders at 440 nm [$\epsilon \approx 11\,400$ (M ferrochelatase)$^{-1}$ cm^{-1}] and 525 nm [$\epsilon \approx 9500$ (M ferrochelatase)$^{-1}$ cm^{-1}] (molar absorptivities are based on protein concentration determinations and a molecular mass of 42 kDa); the absorption ratio A_{440}/A_{278} for this sample was determined to be 0.12. The bands at 330, 440, and 525 nm arise from the $[2Fe-2S]^{2+}$ cluster. As mentioned above, the ratio A_{440}/[Fe] is seen to be constant in all samples, as expected for a visible resonance arising from the [2Fe−2S] cluster, and this suggests that the molar absorptivities should be expressed in the more appropriate units of (M Fe)$^{-1}$ cm^{-1}. When this is done, we find $\epsilon_{330} \approx 15\,000$ (M Fe)$^{-1}$ cm^{-1}, $\epsilon_{440} \approx 8\,000$ (M Fe)$^{-1}$ cm^{-1}, and $\epsilon_{525} \approx 6500$ (M Fe)$^{-1}$ cm^{-1}. Unlike the spectrum of the recombinant human enzymes,[6,11] the spectrum of mouse ferrochelatase does not show a strong absorption at 415 nm. This peak is indicative of a heme contaminant that could not be removed from the human ferrochelatase preparations. The lack of this absorbance indicates that the purified recombinant mouse protein is free of heme contamination.

(19) Ferreira, G. C. *J. Biol. Chem.* **1994**, *269*, 4396−4400.

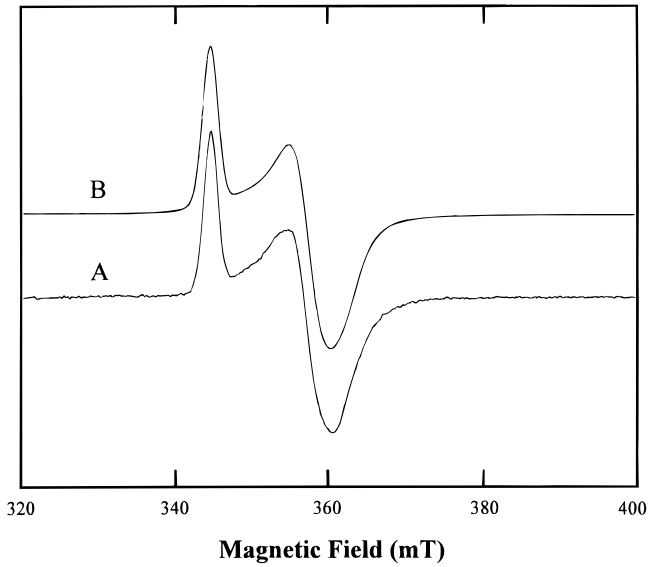

Figure 3. X-Band EPR spectrum of sodium dithionite-reduced protein. Experimental conditions: microwave frequency, 9.6535 GHz; microwave power, 2 mW; $\mathbf{B}_1 \perp \mathbf{B}_0$; temperature, 70 K; instrumental gain, 2 × 10^5; modulation, 1 mT; modulation frequency, 100 kHz. The protein concentration is 70 μM. The solid line B is a theoretical simulation of the experimental spectrum A, calculated using the values in Table 1.

EPR Spectroscopy. The results of initial analyses of EPR spectroscopy of the wild-type mouse ferrochelatases from mouse liver and recombinant *E. coli* sources[5] and recombinant human ferrochelatase[6] have been reported. Here we have conducted a more detailed analysis of the EPR spectra of the recombinant mouse enzyme. The as-isolated recombinant ferrochelatase exhibited no resonances (data not shown). This is as expected for a $[2Fe-2S]^{2+}$ protein, since the cluster exists in a diamagnetic state due to strong antiferromagnetic exchange coupling $J\mathbf{S}_1\cdot\mathbf{S}_2$ between the two high-spin ferric ions.[17] Upon reduction of the cluster by sodium dithionite, a nearly-axial EPR signal is detected in the $g = 2$ region (Figure 3), indicative of a mixed valent $S = {}^1/_2$ system in which $S = 2$ Fe^{2+} ions is antiferromagnetically exchange-coupled to a $S = {}^5/_2$ Fe^{3+} ion. At low temperatures ($T \leq 80$ K), the spectral shape is essentially temperature-independent. The experimental spectrum in Figure 3A was taken at 70 K and is typical of those at low temperature. At low temperatures, the broadness of the spectral lines results from a continuous distribution of microconformational states of the cluster. The resulting line shape is commonly, but not always,[20] modeled with a Gaussian function. The solid line shown in Figure 3B is a theoretical simulation based on the parameters in Table 1 and assumes a Voigt line shape (see below). The low-field resonance ($g = 2.00$) is most nearly Gaussian; the high-field resonance ($g = 1.91$) is least Gaussian, being best simulated with equal width contributions from the Gaussian and Lorentzian components. At temperatures above 140 K, the spectrum begins to broaden noticeably. This phenomenon is due to the increased relaxation rate among the levels of the EPR-active ground Kramers doublet caused by the more efficient relaxation mechanisms that predominate at high temperatures. These mechanisms involve interactions

(20) Gayda, J.-P.; Bertrand, P.; More, C.; LeGall, J.; Cammack, R. C. *Biochem. Biophys. Res. Commun.* **1981**, *99*, 1265−1270.

Table 1. EPR Parameters of $Na_2S_2O_4$-Reduced Ferrochelatase at $T \leq 80$ K

	widths (mT)	
g-values	Gaussian	Lorentzian
2.00	2.2	<0.1
1.93	3.5	0.8
1.91	2.5	2.5

between the spin system and the frozen lattice. Relaxation mechanisms derived from these interactions cause the conformational broadening to be convolved with a new line shape, usually treated as Lorentzian.[21] The absorption shape resulting from this convolution of a Lorentzian broadening function with a Gaussian envelope is known as a Voigt profile. The broadening is proportional to the spin−lattice relaxation rate $1/T_1$. Of the three well-described relaxation processes (the direct mechanism, the Raman mechanism, and the Orbach mechanism),[22] relaxation at high temperatures in Fe−S proteins has been best described by the Orbach process.

Estimation of *J*. At temperatures $T < J/k$, where k is the Boltzmann constant, the strong antiferromagnetic exchange interaction essentially confines the $[2Fe-2S]^+$ cluster to the $S = {}^1/_2$ ground state. In the Orbach mechanism, lattice phonons interact with the Fe−S cluster *via* unoccupied high-energy excited states of the cluster. As the phonons follow a Debye distribution, this process becomes very efficient as the temperature (and hence the density of phonons of proper energy to interact with the excited state) rises. In this model, the relaxation rate, and therefore the broadening, is described by the function

$$1/T_1 = A(e^{\Delta/kT} - 1)^{-1} \quad (1)$$

where Δ is the energy of the lowest excited state and T is the temperature. A fit of the broadened component of the line width to eq 1 will therefore yield the energy Δ of the excited state; for a $S = {}^1/_2$ system, Δ is $3J/2$.

We have used this approach to provide an estimate of J for the dithionite-reduced recombinant mouse ferrochelatase. Spectra were collected in the temperature range 10−220 K. The low melting point of the solubilization medium (≈240 K) precluded extending the measurements to higher temperatures; significant broadening is therefore only observed at the highest temperatures (160, 180, 200, and 220 K). The temperatures were controlled by a liquid-helium flow system (see Experimental Section), and the uncertainty in temperature is therefore expected to be significant, up to 5−10 K (at the temperatures that show broadening, this corresponds to a maximum uncertainty in $1/T$ of only 3×10^{-4} K^{-1}). All spectra were simulated by a computer program which calculates a Voigt profile. The broadened Lorentzian component of the spin−packet line widths were fitted with eq 1. The results are shown in Figure 4 for the well-resolved low-field resonance ($g = 2.00$); the less well-resolved resonances at $g = 1.91$ and 1.93 yielded similar results. From the data in this figure, it is easily seen that this fitting procedure may be used to provide a fairly accurate estimate of the lower limit of Δ. The direct relaxation process, which broadens the lines with a temperature dependence proportional to T_1,[22] is seen to be negligible from the low-temperature points. The system allows us to only record a limited number of broadened points; therefore, we cannot exclude a small contribution from the Raman process in our analysis. However, any contribution to the relaxation from this process would tend to make the apparent value of Δ estimated from our method be smaller than the actual value. Therefore, it is readily seen that the value obtained from our fitting procedure, in which the Raman process is neglected, is a *lower* limit of Δ in which a good deal of confidence can be placed. The good fit seen in Figure 4 lends additional justification to our method. The value obtained from this method, ∼750−1000 cm^{-1}, corresponding to a J of ∼500−650 cm^{-1}, lies at the high end of the range of J in $[2Fe-2S]^+$ clusters measured by this technique.[23,24] We have attempted to fit the double-integrated intensities of the $S = {}^1/_2$ signal with a partition function, $I \propto (1 + 2e^{-\Delta/kT})^{-1}$. The data conformed to a Curie law out to 120 K; above this temperature, the poor signal/noise ratio of the derivative spectrum causes a large uncertainty and precludes such a procedure. Salerno *et al.*[23] observed an empirical relation between the J value and the degree of rhombic distortion of the EPR signal: the higher the J, the more axial the EPR signal. In the ferrochelatase mixed valent cluster, the J value is among the largest observed for this class of diiron center; however, the *g*-values are slightly more rhombic than those of certain other $[2Fe-2S]^+$ clusters with smaller exchange couplings.[23] Therefore, ferrochelatase is somewhat of an exception to this suggested empirical relation.

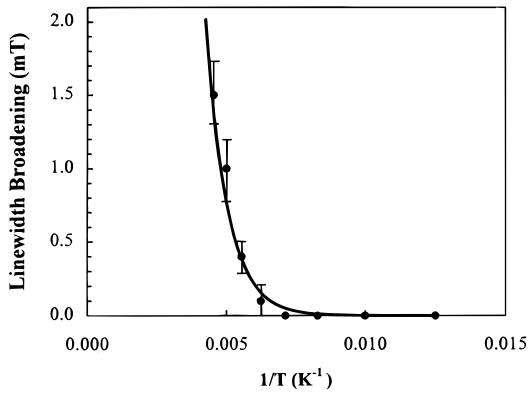

Figure 4. Relaxation broadening of the EPR spectrum. Broadened widths measured on the resolved low-field resonance ($g = 2.00$) as described in the text. The data are fitted with an Orbach model of relaxation [eq 1, solid curve] which yields an exchange coupling constant of ≈590 cm^{-1}. Experimental conditions are as described in the caption for Figure 2, except for the microwave power (see Experimental Section).

Redox Titrations. The midpoint redox potential was determined for the recombinant ferrochelatase $[2Fe-2S]^{2+/+}$ couple by titration followed by both visible and EPR spectroscopy. For the visible titration, the reduction of the cluster was measured by the disappearance of the 510 nm absorbance with decreasing redox potential (Figure 5A). The data were fitted to a Nernst equation curve ($n = 1$), yielding a midpoint potential of −390 ± 10 mV. For the EPR titration, the reduction of the cluster was monitored by following the intensity of the $g = 2.00$ resonance (Figure 5B). A midpoint redox potential of −405 ± 10 mV was obtained, in very good agreement with the value from the visible titration.

Mössbauer Spectroscopy. The presence of a diamagnetic ground state for the $[2Fe-2S]^{2+}$ cluster in recombinant ferrochelatase is established by Mössbauer spectroscopy. We had previously reported that the 4.2 K Mössbauer spectrum of the as-isolated recombinant ^{57}Fe-enriched ferrochelatase demonstrated only a quadrupole doublet with parameters $\Delta E_Q = 0.69 \pm 0.03$ mm/s and $\delta = 0.28 \pm 0.02$ mm/s.[5] In the absence of

(21) Abragam, A.; Bleaney, B. *Electron Paramagnetic Resonance of Transition Ions*; Oxford University Press: London, 1970; p 124.

(22) Gayda, J.-P.; Gibson, J. F.; Cammack, R.; Hall, D. O.; Mullinger, R. *Biochim. Biophys. Acta* **1976**, *434*, 154−163.

(23) Salerno, J. C.; Ohnishi, T.; Blum, H.; Leigh, J. S. *Biochem. Biophys. Acta* **1977**, *494*, 191−197.

(24) Gayda, J.-P.; Bertrand, P.; More, C.; Cammack, R. *Biochimie* **1981**, *63*, 847−849.

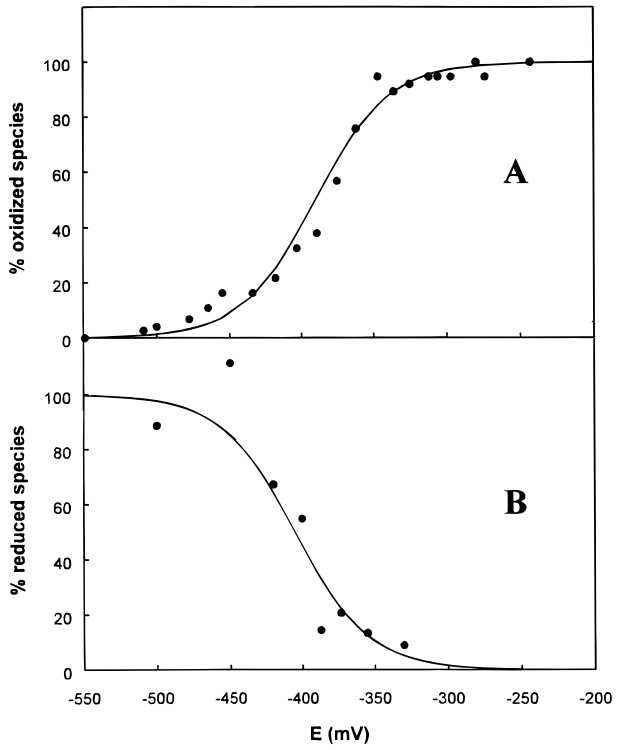

Figure 5. (A) Absorbance change of the ferrochelatase 510 nm visible band as a function of redox potential; (B) intensity of the $g = 2.00$ resonance as a function of redox potential. In both cases, the data were fitted with a one-electron Nernst equation, which yielded a midpoint potential for the [2Fe−2S] cluster of (A) − 390 ± 10 mV and (B) − 405 ± 10 mV.

an external magnetic field, the Mössbauer spectrum of an integer spin system is expected to consist of such quadrupole doublets. In the presence of strong external magnetic fields, however, ^{57}Fe nuclei in a system with integer electronic spin $S \geq 1$ will experience magnetic perturbations from both the external field and the magnetic hyperfine interaction, while ^{57}Fe nuclei in a $S = 0$ system will be subject to perturbation only from the external field. The Mössbauer spectrum of the as-isolated ^{57}Fe-enriched recombinant mouse ferrochelatase at 4.2 K and in the presence of an 8 T magnetic field applied parallel to the propagation direction of the γ-beam is shown in Figure 6. The solid curve in Figure 6 is a theoretical simulation based on the parameters in Table 2 and assumes that the ground electronic state is isolated and diamagnetic.

The $S = {}^1/_2$ sodium dithionite-reduced mixed valent protein was also characterized by Mössbauer spectroscopy. The spectral components originating from the ferric and ferrous sites in the cluster are separately resolved by such a technique. Spectra of the dithionite-reduced ^{57}Fe-enriched recombinant wild-type ferrochelatase are shown in Figure 7. Spectrum A was recorded at 4.2 K in the presence of a 60 mT magnetic field applied parallel to the direction of the γ-beam, while spectrum B was collected under identical conditions but with the field oriented perpendicular to the γ-beam. Spectrum C was collected at 4.2 K and in the presence of an 8 T magnetic field oriented parallel to the γ-beam. The solid curves which overlay the experimental data are theoretical simulations based on the EPR g-values and the parameters listed in Table 2, while the curves plotted above the spectra represent the individual ferric (solid line) and ferrous (dashed line) components. The model used in constructing the simulations assumes a well-isolated $S = {}^1/_2$ ground electronic state (see Barata *et al.*[25] for a description of the $S = {}^1/_2$ spin

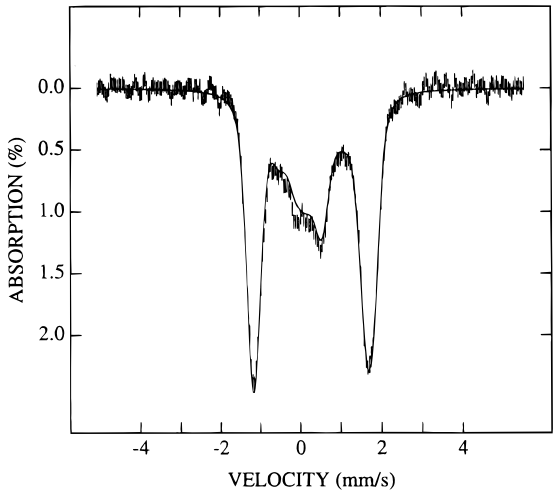

Figure 6. Mössbauer spectrum of as-isolated ^{57}Fe-enriched ferrochelatase. The spectrum was recorded at 4.2 K in the presence of an 8 T magnetic field oriented parallel to the γ-beam. The solid line plotted over the experimental data is a theoretical simulation based on the parameters of Table 2 and assumes an isolated diamagnetic ground state. The protein concentration is 1.6 mM.

Table 2. Mössbauer Parameters for Mouse Ferrochelatase

		$Na_2S_2O_4$ reduced	
	as-isolated	Fe^{3+} site	Fe^{2+} site
δ (mm/s)	0.28 ± 0.02	0.28 ± 0.03	0.67 ± 0.04
ΔE_Q (mm/s)	0.69 ± 0.03	+1.2 ± 0.2	+3.3 ± 0.1
η	0.6 ± 0.2	0 ± 0.3[a]	0 ± 0.2[a]
$A_{\xi\xi}/g_n\beta_n$(T)[b]		−41 ± 1	21.5 ± 0.5
$A_{\sigma\sigma}/g_n\beta_n$(T)[b]		−33.5 ± 1	21.5 ± 0.5
$A_{\zeta\zeta}/g_n\beta_n$(T)[b]		−31.5 ± 1	8.0 ± 0.5
Γ (mm/s)	0.28	0.30	0.30

[a] The EFG tensors of both the ferric site and the ferrous site can be described as axially symmetric with the unique axis in the direction of the smallest magnetic hyperfine component (A-value); this is defined here as the ζ-direction. For both sites, the unique (largest) component of the EFG tensor is positive. [b] The hyperfine constants reported are the effective A-values for the coupled cluster and are related to the intrinsic a-values of the ferric and ferrous ions by $A_{\text{ferric}} = ((\mathbf{S}_{\text{ferric}}\cdot\mathbf{S})/\mathbf{S}^2)\ a_{\text{ferric}} = {}^7/_3\ a_{\text{ferric}}$ and $A_{\text{ferrous}} = ((\mathbf{S}_{\text{ferrous}}\cdot\mathbf{S})/\mathbf{S}^2)\ a_{\text{ferric}} = -{}^4/_3\ a_{\text{ferric}}$. The directions are defined as described in footnote[a] above; the relation to the g-tensor axes cannot be uniquely defined because the principal g-values are approximately isotropic.

Hamiltonian). Certain of the resulting parameters are similar to those reported for other $[2Fe-2S]^+$ cluster in proteins.[25−27] The value of ΔE_Q for the ferric site (1.2 mm/s), however, is the largest value that has been reported for these proteins; the significance of this is not fully understood (see Discussion).

The asymmetric charge distribution of the d^6 high-spin ferrous ion is expected to cause a significant anisotropy in the A-values of this site and also lead to a sizable valence electric field gradient (EFG), which results in a large ΔE_Q.[28] Analysis of the Mössbauer data demonstrates that, for the ferrous ion, both the EFG tensor and the A-tensor have axial symmetry. The unique component of the EFG tensor has a positive sign and corresponds to the same direction as the unique A-tensor component $A_{||}$ (*i.e.*, the unique axes of the two tensors are colinear). The data can only be fit with $A_{||}$ being the component with smallest magnitude.

Attempts to cancel the magnetic hyperfine interaction by increasing the temperature to raise the electronic relaxation rate

(25) Barata, B. A. S.; Liang, J.; Moura, I.; LeGall, J.; Moura, J. J. G.; Huynh, B. H. *Eur. J. Biochem.* **1992**, *204*, 773−778.

(26) Sands, R. H.; Dunham, W. R. *Q. Rev. Biophys.* **1975**, *7*, 443−504.

(27) Münck, E.; Debrunner, P. G.; Tsibris, J. C. M.; Gunsalus, I. C. *Biochemistry* **1972**, *11*, 855−863.

(28) Huynh, B. H.; Kent, T. A. In *Advances in Inorganic Biochemistry*; Eichhorn, G. L., Marzilli, L. G., Eds.; Elsevier Science Publishing Co.: New York, 1984; Vol. 6, pp 163−223.

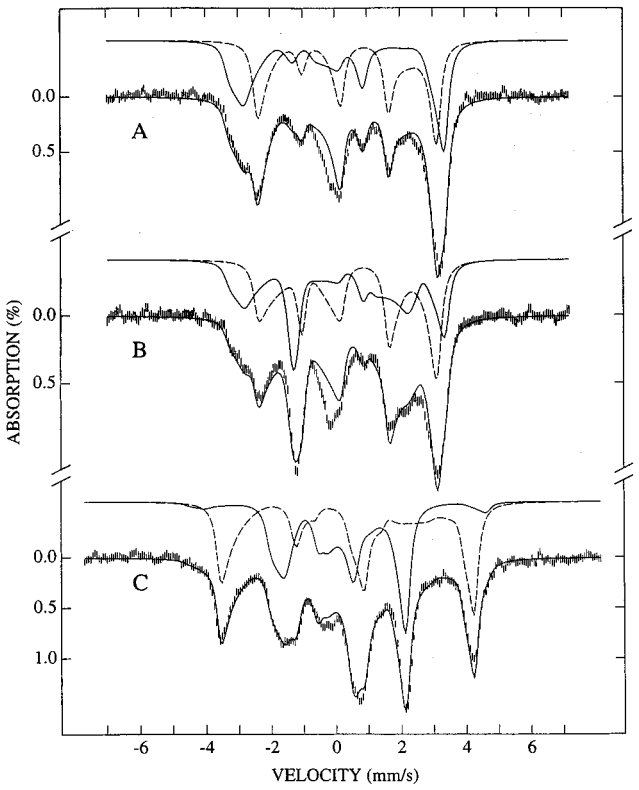

Figure 7. Mössbauer spectrum of sodium dithionite-reduced ^{57}Fe-enriched ferrochelatase. All spectra were recorded at 4.2 K. Spectrum A was collected in the presence of a 60 mT magnetic field oriented parallel to the γ-beam; in spectrum B the 60 mT field was perpendicular to the γ-beam. Spectrum C was collected in the presence of an 8 T field parallel to the γ-beam. Solid lines plotted over the experimental spectra are theoretical simulations calculated assuming an isolated $S = {}^1/_2$ ground state and slow electronic relaxation and using the parameters of Table 2. Lines above the spectra indicate the individual ferric (solid line) and ferrous (dashed line) components. The protein concentration is 1.1 mM.

were not successful: the spectrum did not collapse into quadrupole doublets at temperatures as high as 220 K (data not shown). This is rather unusual behavior for a [2Fe−2S] protein and is another indication of the slow, inefficient Orbach relaxation arising from the strong exchange interaction within the coupled cluster. The $[2Fe-2S]^+$ cluster in adrenal ferredoxin, another mammalian protein with a strong exchange interaction ($J \approx 330-540$ cm^{-1}),[22,23,29] also failed to collapse into quadrupole doublets at temperatures up to 244 K.[30]

Discussion

The recent surprise discovery of a [2Fe−2S] cluster in mammalian ferrochelatases has generated many interesting ideas about this enzyme and its mechanisms of catalytic activity and regulation. Likewise, it has opened new questions regarding the general roles of iron−sulfur clusters in protein chemistry. These cofactors have been shown to have a multitude of functional roles in proteins. An example is the cytosolic aconitase/iron regulatory protein,[31] in which a [4Fe−4S] cluster has both a catalytic and a regulatory role (interconversion of the two functional forms of the protein is mediated by the cluster).[32,33] In the DNA repair enzyme endonuclease III, a [4Fe−4S] cluster is present but is apparently not directly involved in catalysis;[34] its function remains uncertain but a structural role has been proposed.[35] The SoxR protein of *E. coli* has recently emerged as a [2Fe−2S] cluster-containing protein in which the cluster plays an important regulatory role: the protein, a homodimer which activates transcription of the *soxS* gene in response to oxidative stress, appears to need the cluster in order to function as a transcriptional activator.[36] The NifU protein, which has been implicated in the assembly of the Fe-containing cofactors of *Azotobacter vinelandii* nitrogenase,[37] and the *bioB* gene product,[38] which is involved in biotin synthesis, have been recently found to contain [2Fe−2S] clusters of unknown function. Likewise, the role of the iron−sulfur cluster in bacterial L-serine dehydratases has yet to be established.[39,40] The [2Fe−2S] cluster in cytidine 5′-diphosphate-(CDP)-6-deoxy-L-threo-D-glycero-4-hexulose-3-dehydrase, a pyridoxamine 5′-phosphate-dependent enzyme involved in the synthesis of the deoxysugar CDP-ascarylose, is thought to be involved in catalytic electron transfer.[41] In ferrochelatase, the [2Fe−2S] cluster might have a catalytic, redox, regulatory, or structural capacity, or some combination of these. We consider it unlikely that the [2Fe−2S] cluster plays a direct role in catalysis; if so, the yeast and bacterial enzymes, which are not iron−sulfur proteins[6] but do exhibit strong amino acid sequence homology[1] and striking biochemical similarities[2] to the mammalian ferrochelatases, would have a different molecular mechanism from the mammalian enzymes. The possibility exists that the mammalian ferrochelatases are multifunctional enzymes; recent studies have shown that ferrochelatase can bind RNA, possibly indicating a second capacity for the protein.[42] The data of Figure 1, however, do show that the cluster is necessary for ferrochelatase activity. The significance of the nonlinear relationship between the cluster content and the specific activity is currently unclear, but as mentioned above may indicate the presence of multimeric structures in the active enzyme. Radiation inactivation studies have suggested that ferrochelatase is active as a homodimer,[43] and the notion that the enzymatically active ferrochelatase is a homodimer has been invoked as a possible explanation of the dramatic reduction in ferrochelatase activity in some patients with the disease protoporphyria.[6] Investigating the origins of the behavior shown in Figure 1 and elucidation of the functional role of the [2Fe−2S] cluster are primary goals in our study of ferrochelatase.

The study reported here, together with the earlier work,[5,6] currently make the [2Fe−2S] cluster in ferrochelatase the most comprehensively characterized of the [2Fe−2S] clusters in mammalian proteins. It is clear that there are many similarities among the iron−sulfur centers in these proteins, and the

(29) Kimura, T.; Tasaki, A.; Watari, H. *J. Biol. Chem.* **1970**, *245*, 4450−4452.
(30) Cammack, R.; Rao, K. K.; Hall, D. O.; Johnson, C. E. *Biochem. J.* **1971**, *125*, 849−856.
(31) Kennedy, M. C.; Mende-Mueller, L.; Blondin, G. A.; Beinert, H. *Proc. Natl. Acad. Sci. U.S.A.* **1992**, *89*, 11730−11734.
(32) Haile, D. J.; Rouault, T. A.; Harford, J. B.; Kennedy, M. C.; Blondin, G. A.; Beinert, H.; Klausner, R. D. *Proc. Natl. Acad. Sci. U.S.A.* **1992**, *89*, 11735−11739.
(33) Philpott, C. C.; Haile, D.; Rouault, T. A.; Klausner, R. D. *J. Biol. Chem.* **1993**, *268*, 17655−17658.
(34) Cunningham, R. P.; Asahara, H.; Bank, J. F.; Scholes, C. P.; Salerno, J. C.; Surerus, K.; Münck, E.; McCracken, J.; Peisach, J.; Emptage, M. H. *Biochemistry* **1989**, *28*, 4450−4455.
(35) Kuo, C.-F.; McRee, D. E.; Fisher, C. L.; O'Handley, S. F.; Cunningham, R. P.; Tainer, J. A. *Science* **1992**, *258*, 434−440.
(36) Hidalgo, E.; Bollinger, J. M.; Bradley, T. M.; Walsh, C. T.; Demple, B. *J. Biol. Chem.* **1995**, *270*, 20908−20914.
(37) Fu, W.; Jack, R. F.; Morgan, T. V.; Dean, D. R.; Johnson, M. K. *Biochemistry* **1994**, *33*, 13455−13463.
(38) Sanyal, I.; Cohen, G.; Flint, D. H. *Biochemistry* **1994**, *33*, 3625−3631.
(39) Grabowski, R.; Hofmeister, A. E. M.; Buckel, W. *Trends Biochem. Sci.* **1993**, *18*, 297−300.
(40) Grabowski, R.; Buckel, W. *Eur. J. Biochem.* **1991**, *199*, 89−94.
(41) Thorson, J. S.; Liu, H.-W. *J. Am. Chem. Soc.* **1993**, *115*, 7539−7540.
(42) Ferreira, G. C. *Biochem. Biophys. Res. Commun.* **1995**, *214*, 875−878.
(43) Straka, J. G.; Bloomer, J. R.; Kempner, E. S. *J. Biol. Chem.* **1991**, *266*, 24637−24641.

Table 3. Electronic and Nuclear Parameters for Some Mixed Valent [2Fe−2S] Proteins[a]

protein[b]	*g*-values	J (cm^{-1})	$A_{ii}/g_n\beta_n$ (T)	ΔE_Q (mm/s)	η	δ (mm/s)	ref
Sp Fd	1.89, 1.96, 2.05	200	−37.5, −36.1, −30.9	0.64	−0.6	0.25	44,45
		180	8.2, 12.3, 25.9	−3.00	0	0.54	
Py Fd	1.90, 1.96, 2.05		−37.2, −33.7, −30.6	0.68	−0.9	0.25	44
			8.2, 10.2, 24.5	−3.00	0	0.54	
Sl Fd	1.89, 1.96, 2.05		−37.6, −36.5, −30.6	0.60	−0.3	0.27	46
			9.5, 10.9, 26.6	−3.20	0	0.54	
Hh Fd	1.89, 1.98, 2.07	150					23
Sm Fd	1.88, 1.95, 2.04	170					22
Dg AO	*c*		−38.0, −32.0, −30.0	1.0	0	0.30	25
			8.0, 8.0, 22.0	−3.6	−1.5	0.62	
Tt Rp	1.80, 1.90, 2.02		−40.1, −36.5, −31.3	0.63	0	0.31	47
			8.0, 10.2, 24.1	−3.05	−3	0.74	
Ph Rp	nr	130					23
Mt Rd	1.86, 1.96, 2.05		−39.0, −35.6, −31.4	0.59	0	0.31	48
			10.0, 10.8, 26.6	−3.00	0.96	0.65	
Pp Fd	1.94, 1.94, 2.01	*d*	−41.2, −36.8, −31.6	0.6	0.5	0.35	27
			10.3, 15.5, 25.8	−2.7	−3	0.65	
Ma Fd[e]	1.93, 1.94, 2.02	330					24
		540					23
Mo FC	1.91, 1.93, 2.00	570	−41.0, −33.5, −31.5	1.2	0	0.28	
			21.5, 21.5, 8.0	3.3	0	0.67	*f*

[a] For each protein entry, the first line of values are for the Fe^{3+} site and the second for the Fe^{2+} site. Mössbauer hyperfine values are measured at 4.2 K. When more than one J value is quoted, the values represent measurements by different groups. J is in cm^{-1}; $A_{ii}/g_n\beta_n$ is T; and ΔE_Q and δ are in mm/s; nr, not reported. [b] Key: Sp Fd, spinach ferredoxin (Fd); Py Fd, parsley Fd; Sl Fd, *Synechococcus lividus* (algal) Fd; Hh Fd, *Halobacterium halobium* Fd; Sm Fd, *Spirulina maxima* Fd; Dg AO, *D. gigas* aldehyde oxidoreductase; Tt Rp, *Thermus thermophilus* Rieske protein; Ph Rp, pigeon heart Rieske protein; Mt Rd, *Methylosinus trichosporium* OB3b methane monooxygenase reductase; Pp Fd, *P. putida* Fd; Pa Fd, mammalian adrenal gland Fd; Mo FC, mouse ferrochelatase. [c] *D. gigas* aldehyde oxidoreductase contains two [2Fe−2S] clusters; the *g*-values are not reported here and the Mössbauer analysis was treated as an average of the two centers. [d] Salerno *et al.*[23] estimated a value of 450−650 cm^{-1} for J in Pp Fd from the temperature dependence of the Mössbauer spectra of Münck *et al.*[27] [e] A rudimentary analysis of the Mössbauer spectra of mixed valent pig adrenal Fd at 4.2 K has been done by Cammack *et al.*[30] The spectrum did not collapse into quadrupole doublets at temperatures up to 244 K. [f] Present work.

ferrochelatase cluster shares many common features with the other members of this class. Emerging from this characterization, however, are certain properties that are (as yet) unique to ferrochelatase. For comparison, Table 3 lists the spin Hamiltonian parameters of the other well-characterized $[2Fe-2S]^+$ proteins[22−25,27,44−48] alongside those of mouse ferrochelatase.

As previously reported,[5] iron and labile sulfide determinations have again shown substoichiometric quantities of these elements, although the Fe:protein ratios have improved significantly over our earlier work and approach 1 cluster/protein for the "purest" fractions. This increase has aided in spectroscopic investigation of the cluster.

The UV−vis band positions are typical of $[2Fe-2S]^{2+}$ cluster-containing proteins, although the ϵ values are substantially higher here. For the recombinant human ferrochelatase, $\epsilon_{330} \approx 24\,000$ (M protein)$^{-1}$ cm^{-1}, $\epsilon_{460} \approx 11\,000$ (M protein)$^{-1}$ cm^{-1}, and $\epsilon_{550} \approx 9000$ (M protein)$^{-1}$ cm^{-1};[6] these values were described as being roughly 50% larger than those of other $[2Fe-2S]^{2+}$ proteins [reported values for other $[2Fe-2S]^{2+}$ proteins range from 11000−16000 (M protein)$^{-1}$ cm^{-1} for ϵ_{330}, 6000−11000 (M protein)$^{-1}$ cm^{-1} for ϵ_{450}, and 3000−6000 (M protein)$^{-1}$ cm^{-1} for ϵ_{550}]. While our ϵ values for the sample in Figure 2 agree in large part with those of the human ferrochelatase, we reiterate that this sample contains only 0.72 cluster/protein. Scaling our molar absorptivities to 1 cluster/protein, we expect that for a "pure" holoprotein sample $\epsilon_{330} \approx 30\,000$ (M protein)$^{-1}$ cm^{-1}, $\epsilon_{440} \approx 16\,000$ (M protein)$^{-1}$ cm^{-1}, and $\epsilon_{525} \approx 13\,000$ (M protein)$^{-1}$ cm^{-1}. These values are substantially larger than those of other biological $[2Fe-2S]^{2+}$ systems.

The redox properties and spin states of the oxidized and reduced proteins are clearly representative of the [2Fe−2S] class. The midpoint redox potential lies toward the lower end of the range of −240 to −460 mV reported for [2Fe−2S] clusters with all-cysteine coordination.[10] Whether this redox couple is significant in mammalian ferrochelatase is not clear, however, since electron transfer is not a necessary step in the enzymatic mechanism and the $[2Fe-2S]^{2+}$ cluster remains in the oxidized [2Fe−2S] state during turnover conditions.[5] As in other proteins of this group, the electronic relaxation rates for the mixed valent state as measured by EPR spectroscopy are adequately described by considering only the Orbach relaxation process. This allows an estimate of the size of the antiferromagnetic exchange coupling constant J. The estimated value of ∼500−650 cm^{-1} is large for a $[2Fe-2S]^+$ protein, but not excessively so.

Certain other characteristics of the ferrochelatase cluster, however, make it unique among the [2Fe−2S] cluster-containing proteins. The hyperfine interactions in the mixed valent ferrochelatase cluster, as measured by Mössbauer spectroscopy and summarized in Table 2, are not identical to those in other characterized $[2Fe-2S]^+$ clusters. The Mössbauer spectra are fit best with an axially symmetric EFG tensor for the ferrous ion. The EFG component of the largest magnitude has a positive sign and is large compared to those of the most other proteins in this class. The spectra are also fit best with an axially symmetric ferrous A-tensor, with the unique component $A_{||}$ the smallest in magnitude. Axial or near-axial symmetry of the ferrous ion A-tensor in $[2Fe-2S]^+$ proteins has been reported;[25,44,47,48] however, in the usually observed case $A_{||}$ has the largest magnitude of the A-values. The ferrochelatase [2Fe−2S] cluster seems to be unique in this regard. The direction of $A_{||}$ for the ferrous ion is parallel to the unique EFG component; however, a correlation of the directions of the principal g-tensor

(44) Dunham, W. R.; Bearden, A. J.; Salmeen, L. T.; Palmer, G.; Sands, R. H.; Orme-Johnson, W. H.; Beinert, H. *Biochim. Biophys. Acta* **1971**, *253*, 134−152.
(45) Palmer, G.; Dunham, W. R.; Fee, J. A.; Sands, R. H.; Iizuka, T.; Yonetani, T. *Biochim. Biophys. Acta* **1971**, *245*, 201−207.
(46) Anderson, R. E.; Dunham, W. R.; Sands, R. H.; Bearden, A. J.; Crespi, H. L. *Biochim. Biophys. Acta* **1975**, *408*, 306−318.
(47) Fee, J. A.; Findling, K. L.; Yoshida, T.; Hille, R.; Tarr, G. E.; Hearshen, D. O.; Dunham, W. R.; Day, E. P.; Kent, T. A.; Münck, E. *J. Biol. Chem.* **1984**, *259*, 124−133.
(48) Fox, B. G.; Hendrich, M. P.; Surerus, K. K.; Anderson, K. K.; Froland, W. A.; Lipscomb, J. D.; Münck, E. *J. Am. Chem. Soc.* **1993**, *115*, 3688−3701.

Table 4. Calculated Magnetic Hyperfine Parameters for the Fe^{2+} Site in the Ferrochelatase $[2Fe-2S]^+$ Cluster[a]

	calculation	experiment
$A_{xx}/g_n\beta_n$ (T)	21.6	21.5
$A_{yy}/g_n\beta_n$ (T)	7.6	8.0
$A_{zz}/g_n\beta_n$ (T)	21.6	21.5

[a] The intrinsic *a*-values are calculated as in Bertrand and Gayda[50,51] with the ground state defined in eq 2 and $\theta = -27.5°$. The values listed in this table are the effective *A*-values for the coupled $[2Fe-2S]^+$ cluster (see footnote b of Table 2). The parameters used in the calculations are $P = 55$ MHz; $\kappa = 0.39$; energy separations, $\Delta_{xy} = 2000\ cm^{-1}$, $\Delta_{xz} = 6000\ cm^{-1}$, $\Delta_{yz} = 4000\ cm^{-1}$; $\lambda = -80\ cm^{-1}$. Note that the directions of the principal axes have been redefined relative to those of Table 2 in order to keep $|xy\rangle$ the lowest excited state in the calculations of this table; the correspondence between the two axis systems is $x \rightarrow \sigma$, $y \rightarrow \zeta$, and $z \rightarrow \xi$.

axes and the *A*-tensor and EFG tensor axes could not be made, since the Mössbauer spectra are not sufficiently sensitive to small variations in the cluster *g*-values, all of which are near 2.0. ENDOR measurements could perhaps clarify this situation.

The value of g_{av} in the mixed valent cluster of 1.94 places it best into the "ferredoxin"-type of [2Fe−2S] cluster, with $g_{av} = 1.96$, as opposed to the "Rieske"-type of cluster, with $g_{av} = 1.91$.[49] Bertrand and Gayda[50] have developed a model to describe the properties of such clusters that is defined by the ground state of the sixth electron of the d^6 ferrous ion. In a distorted tetrahedral environment, this ground state is hypothesized to be a mixture of $d_{x^2-y^2}$ and d_{z^2} states, defined as

$$|\varphi_0\rangle = \cos\theta\,|z^2\rangle + \sin\theta\,|x^2 - y^2\rangle \qquad (2)$$

Within this state, and with the ferric ion postulated to be ^6S, the electronic and nuclear parameters (EFG and magnetic hyperfine tensor components) of the ferrous ion and the *g*-values of the $[2Fe-2S]^+$ cluster can be calculated. It is found that this model predicts with reasonable accuracy the symmetry and sign of the ferrous *A*-tensor and EFG tensor elements for a value θ of approximately $-30°$.[50,51] For this ground state, the EFG tensor of the ferrous ion is axially symmetric and the unique component is predicted to have a positive value $4|e|\langle r^{-3}\rangle(1 - R_0)/7$. Its *A*-tensor also exhibits nearly-axial symmetry with the unique component $A_{||}$ being the smallest in magnitude, and the direction of $A_{||}$ for the ferrous ion is parallel to the unique EFG component. The *A*-values calculated from this model are listed along with the experimental values in Table 4. The best match of the experimental data is achieved if the contact factor κ is chosen as 0.39, instead of its usually assumed value of 0.35, with a mixing angle θ of $-27.5°$. The minor deviation of κ should not be considered a major difficulty in this relatively crude model. Conversely, the values of the parameters deduced from this simple model should also not be taken literally.

The Fe^{3+} site in the mixed valent cluster also exhibits some unusual properties. The ferric *A*-tensor is found to have a fair amount of anisotropy, and as noted above, the ΔE_Q for this site is the largest reported for $[2Fe-2S]^+$ clusters. The value of ΔE_Q is determined by the superposition of the EFGs at the nucleus generated by the Fe valence electrons and the ligand charge distribution. To a first approximation, the ferric ion has a ^6S state with a spherical electronic distribution and should therefore have no valence EFG. The large value of ΔE_Q for this ion implies that the surrounding geometry is strained or asymmetrical, resulting in a relatively large ligand EFG and perhaps causing the ferric ion ground state to deviate from a pure ^6S character, yielding a nonzero valence EFG. The observed anisotropy in the ferric ion *A*-tensor is furthermore not a property of the ^6S state, although significant anisotropy in these values (± approximately 15% of the average value) has been documented for other $[2Fe-2S]^+$ proteins.[25,27] This may be attributable to a high degree of covalency with the ligand sulfurs or to a sizable distortion from a purely tetrahedral arrangement of ligand charge density. It is not clear why the ΔE_Q of the ferric ion changes so dramatically upon reduction of the cluster (from 0.7 mm/s in the oxidized cluster to 1.2 mm/s in the mixed valent cluster), since the electronic state of the Fe^{3+} site should not be directly affected by the addition of an electron to the other iron to form the localized Fe^{2+} site. Usually, the ferric ion ΔE_Q in the mixed valent state does not differ appreciably from that of the oxidized state.[27,44,47] There may well be some ligand rearrangement for the entire cluster that takes place upon reduction. An attempt to reoxidize a mixed valent sample in order to test whether the cluster would reversibly convert to the original "native" ligand arrangement in the $[2Fe-2S]^{2+}$ form resulted in precipitation of the protein.

Finally, we consider the protein structure. A comparison of the primary structures of mammalian ferrochelatases with other [2Fe−2S] proteins yields another difference between ferrochelatase and the other proteins in this class. In ferrochelatase, the four putative cluster-binding cysteines are found in a 30-residue tail near the C-terminus in a sequence Cys-X_7-Cys-X_2-Cys-X_4-Cys. This type of sequence is unique among [2Fe−2S] cluster-containing enzymes in that it only involves a small portion of the polypeptide chain: the cysteines are spaced over only 17 out of *ca*. 400 residues in the mature protein. In fact, all the reported cases of [2Fe−2S] clusters with four binding cysteines have a X_n spacing between neighboring cysteines where $n \geq 29$: Cys-X_4-Cys-X_2-Cys-X_{29}-Cys for plant-type ferredoxins;[52,53] Cys-X_5-Cys-X_2-Cys-X_{35-37}−Cys for adrenal or *Pseudomonas putida* ferredoxins;[54−56] Cys-X-Cys-X_{32}-Cys-X_2-Cys for the *A. vinelandii* NifU protein;[37] Cys-X_2-Cys-X_{33}-Cys-X-Cys for the center II domain of *Desulfovibrio gigas* aldehyde oxidoreductase.[57,58] Such close spacing of the ligand cysteines in mammalian ferrochelatases may have implications for any putative structural function for the cluster: whereas the clusters in other [2Fe−2S] proteins with all-cysteine protein coordination link distant regions of the protein primary structure, the ferrochelatase cluster does not. Interestingly, a remarkably similar spacing (Cys-X_6-Cys-X_2-Cys-X_5-Cys) is observed in the unique cysteine ligand pattern for the [4Fe−4S] cluster of endonuclease III.[35] The X-ray structure of this protein reveals that a 26-residue carboxy-terminus loop forms a right-handed spiral around the cluster; the role of the cluster was proposed to involve the correct positioning of conserved basic residues for interaction with the DNA phosphate backbone. Whether the unique amino acid sequence of the binding cysteines in mammalian ferrochelatase has a similar importance to that

(49) Bertrand, P.; Guigliarelli, B.; More, C. *New J. Chem*. **1991**, *15*, 445−454.
(50) Bertrand, P.; Gayda, J.-P. *Biochim. Biophys. Acta* **1979**, *579*, 107−121.
(51) The Hamiltonian used in ref 50 for the electronic nuclear hyperfine coupling has a sign that is opposite to convention. The intrinsic *a* values calculated by their formulas therefore are positive instead of negative.
(52) Tsukihara, T.; Fukuyama, K.; Mizushima, M.; Harioka, T.; Kusunoki, M.; Katsube, Y.; Hase, T.; Matsubara, H. *J. Mol. Biol*. **1990**, *216*, 399−410.
(53) Jacobson, B. L.; Chae, Y. K.; Markley, J. L.; Rayment, I.; Holden, H. M. *Biochemistry* **1993**, *32*, 6788−6793.
(54) Cupp, J. R.; Vickery, L. E. *J. Biol. Chem*. **1988**, *263*, 17418−17421.
(55) Gerber, N. C.; Horiuchi, T.; Koga, H.; Sligar, S. G. *Biochem. Biophys. Res. Commun*. **1990**, *169*, 1016−1020.
(56) Uhlmann, H.; Beckert, V.; Schwarz, D.; Bernhardt, R. *Biochem. Biophys. Res. Commun*. **1992**, *188*, 1131−1138.
(57) Thoenes, U.; Flores, O. L.; Neves, A.; Devreese, B.; Van Beeumen, J. J.; Huber, R.; Romão, M. J.; LeGall, J.; Moura, J. J. G.; Rodrigues-Pousada, C. *Eur. J. Biochem*. **1994**, *220*, 901−910.
(58) Romão, M. J.; Archer, M.; Moura, I.; Moura, J. J. G.; LeGall, J.; Engh, R.; Schneider, M.; Hof, P.; Huber, R. *Science* **1995**, *270*, 1170−1176.

proposed for endonuclease III, or some other structural significance, is currently unknown. Comparative, direct structural studies, such as X-ray diffraction experiments currently under way, may shed light on the differences between the ferrochelatase cluster and other [2Fe−2S] clusters and aid in the determination of the function of the cluster.

In conclusion, we have spectroscopically characterized the [2Fe−2S] cluster in mammalian ferrochelatase. The physicochemical properties of the cluster are, with notable exceptions, in many ways similar to those of other protein [2Fe−2S] clusters. The cluster appears to be necessary for activity, although the exact nature of this role is yet to be determined. Further studies are needed to fully elucidate the molecular mechanism of ferrochelatase catalysis and to define the role of the [2Fe−2S] cluster in the mammalian enzyme.

Experimental Section

Reagents. Blue Sepharose CL-6B was obtained from Pharmacia/LKB Biotechnology. Deuteroporphyrin IX dihydrochloride was purchased from Porphyrin Products. Bicinchoninic acid protein assay reagents were obtained from Pierce Chemical Company. ^{57}Fe metal foil (>95% pure) was from Advanced Materials and Technology. The metallic iron was dissolved into dilute H_2SO_4 as described previously.[59] Natural-abundance ferrous ammonium sulfate and sodium citrate were from Fisher Scientific. L-Ascorbic acid, 2,4,6-tripyridyl-(*S*)-triazine (TPTZ), and a ferric standard solution were from Sigma. All other chemicals were of the highest purity available.

Enzyme Preparation. Recombinant murine liver ferrochelatase was isolated from hyperproducing *E. coli* cells containing the plasmid pGF42.[19] Cells were grown in a rich medium containing natural-abundance iron (2.2% ^{57}Fe) or, alternatively, in a minimal medium containing 20 μM, 95%-enriched ^{57}Fe. The protein was purified and concentrated as described previously[5] with the modification that the buffers used throughout the process did not contain dithiothreitol. No special anaerobic techniques were used at this stage; the protein was purified and concentrated in air. The purified, concentrated protein (typically 1−2 mM) was frozen and stored in liquid nitrogen until use. Activity assays were conducted anaerobically in a 0.1 M Tris·HCl, pH = 8.5 buffer solution and without reducing agents as described previously.[14] Reduction of the [2Fe−2S] cluster was accomplished by addition of a strongly buffered sodium dithionite solution.

Chemical Analysis. Initially, protein iron concentrations were determined by both inductively coupled plasma emission spectroscopy (conducted using a Jarrel−Ash AtomComp 965 spectrometer) and a colorimetric assay using the ferrous-chelating chromophore 2,4,6-tripyridyl-(*S*)-triazine (TPTZ).[60] The two methods gave identical results, and subsequently all iron determinations were done using only the TPTZ method. Likewise, protein concentrations were initially determined by amino acid analysis (Institut fuer Reproduktionsmedizin, Tieraerztliche Hochschule, Hannover, Germany) and also by the bicinchoninic acid assay using bovine serum albumin as the standard.[61] After confirmation that both methods gave similar results, only the bicinchoninic acid assay was used. Acid-labile sulfide measurements were performed according to the method of Fogo and Popowsky[62] as modified by Beinert.[63]

EPR Spectroscopy. EPR spectra were recorded with a Bruker ER 200D-SRC spectrometer operating in X-band and equipped with an Oxford Instruments ESR 910 continuous flow cryostat. Spectra were recorded in both the as-isolated and the sodium dithionite-reduced states.

In order to obtain an estimate of the magnitude of the exchange interaction, EPR spectra of the dithionite-reduced protein were collected in the temperature range of 10−220 K. The low-temperature (T < 60 K) power-saturation properties of the reduced cluster were first determined, and for these temperatures the spectra were collected under nonsaturating conditions (microwave powers were as follows: 10 K, 2 μW; 20 K, 63 μW; 30 K, 200 μW; 40 K, 630 μW; 50−80 K, 2 mW; 100−140 K, 6.3 mW; 160−200 K, 20 mW; 220 K, 200 mW). The spectral line widths are broadened by the more efficient relaxation mechanisms that dominate at higher temperatures. The widths were measured by spectral simulation, and the values were fitted with an Orbach relaxation model. This procedure allows an estimate of the energy of the lowest exchange-coupled excited state.[22]

Visible Redox Titration. The protein was diluted into a 20 mM Tris·HCl, pH = 8.0 buffer containing 20% glycerol, 1.5 M NaCl and 1% sodium cholate, to a final absorbance of 0.17 at 510 nm. The following mediators were present at a concentration of 10 nM each: phenazine ethosulfate ($E_0' = 55$ mV), Methylene Blue ($E_0' = 11$ mV), Indigo Carmine ($E_0' = -111$ mV), anthraquinone-1,5-disulfonic acid ($E_0' = -325$ mV), phenosafranine ($E_0' = -255$ mV), Safranine-O ($E_0' = -280$ mV), neutral red ($E_0' = -325$ mV), methyl viologen ($E_0' = -436$ mV), and *m*-dimethyltriquat ($E_0' = -617$ mV). Potentials were measured using a platinum electrode as the working electrode and a saturated calomel electrode as the reference and are quoted relative to the normal hydrogen electrode. The cell was calibrated with a standard solution of 50 mM $K_3Fe(CN)_6/K_4Fe(CN)_6$ in 0.1 M K_3PO_4 at pH 7.0. The reduction was obtained by addition of aliquots of a 1 mg/mL sodium dithionite solution. The titration was followed by measuring the absorption at 510 nm.[64]

EPR Redox Titration. The procedure for the EPR redox titration is essentially the same as that for the visible titration. The protein was diluted in the same buffer as in the visible titration to a final concentration of 120 μM. Mediators were the same as in the visible titration except that their concentrations were 40 μM each. The titration was accomplished inside an anaerobic chamber described previously,[65] and the sample was transferred to a quartz EPR sample tube without exposure to air. The working electrode in this case was a gold coil, and a Ag/saturated AgCl system served as the reference electrode. The titration was followed by measuring the intensity of the $g = 2.00$ resonance.

Mössbauer Spectra. Spectra were recorded on a constant acceleration spectrometer. The instrument is equipped with a Janis 8DT variable temperature controller. Spectra were collected in the temperature range 4.2−220 K and in the absence or presence of a magnetic field range of 60 mT to 8 T which can be applied either parallel or perpendicular to the direction of propagation of the γ-beam. The zero velocity of the Mössbauer spectra is referenced to the centroid of the room temperature spectrum of a metallic iron foil.

UV−Visible Spectroscopy. Absorption spectra were recorded on a Shimadzu UV-2101PC spectrophotometer or, alternatively, on a Perkin-Elmer Lambda 2 spectrometer.

Acknowledgment. We thank Dr. Juan Calvete at Institut fuer Reproduktionsmedizin, Tieraerztliche Hochschule, Hannover, Germany, for his assistance in the amino acid determination. This work was supported by National Institutes of Health grants GM47295 and GM51977 (B.H.H.), by American Heart Association Florida Affiliate (no. 9501372) and National Science Foundation Young Investigator Award MCB-9257656 (G.C.F.), by grant CRG 921238 from NATO (G.C.F. and I.M.), and by grants PBIC/QUI/1646/93 (I.M.) and PBIC/BIO/1668/93 (J.J.G.M.). Mr. S. G. Lloyd is a recipient of a Young Scientist Training Scholarship from the Life and Health Insurance Medical Research Fund. Dr. R. Franco is a recipient of an INVOTAN Research Scholarship.

JA954000O

(59) Ravi, N.; Bollinger, J. M.; Huynh, B. H.; Edmondson, D. E.; Stubbe, J. *J. Am. Chem. Soc.* **1994**, *116*, 8007−8014.
(60) Fischer, D. S.; Price, D. C. *Clin. Chem.* **1964**, *10*, 21−31.
(61) Smith, P. K.; Krohn, R. I.; Hermanson, G. T.; Mallia, A. K.; Gartner, F. H.; Provenzano, M. D.; Fujimoto, E. K.; Goeke, N. M.; Olson, B. J.; Klenk, D. C. *Anal. Biochem.* **1985**, *150*, 76−85.
(62) Fogo, J. K.; Popowski, M. *Anal. Chem.* **1949**, *21*, 732−734.
(63) Beinert, H. *Anal. Biochem.* **1983**, *131*, 373−378.
(64) Huang, J. J.; Kimura, T. *Biochemistry* **1973**, *12*, 406−409.
(65) Gupta, N.; Bonomi, F.; Kurtz, D. M.; Ravi, N.; Wang, D. L.; Huynh, B. H. *Biochemistry* **1995**, *34*, 3310−3318.